

Full Paper | <http://dx.doi.org/10.17807/orbital.v16i4.21957>

Lignocellulosic Biomass Derived Carbon Supported Nickel Nanoparticles as an Efficient Catalyst for Reduction of Nitroarenes

Sunshine Dominic Kurbah* ^a, Kenneth Umdor ^b, and Ndege Simisi Clovis ^c

Nickel-based catalysts directing selectivity for the reduction of nitroarenes reduction have drawn a lot of attention; yet, they have not yielded considerable accomplishments. Here, we report an environmentally friendly method for synthesizing a nickel-based carbon-supported nanocatalyst that is easily synthesized using lignin residues. The carbon-supported nickel nanoparticle catalysts generated from lignocellulosic biomass were characterized by powder x-ray diffraction (XRD), energy-dispersive x-ray spectroscopy (EDS), and transmission electron microscopy (TEM). The present catalytic system not only shows outstanding performance with an excellent anilines output but also shows an environmentally friendly catalytic process with simple separation, easy operations, reuse and recycle.

Graphical abstract



Keywords

Biomass
Lignocellulosic
Nickel nanoparticles
Nitroarenes
Reduction

Article history

Received 20 Sep 2024
Revised 16 Dec 2024
Accepted 27 Dec 2024
Available online 09 Jan 2025

Handling Editor: Ana C. Micheletti

1. Introduction

A number of hazardous chemicals that have been leaked from industrial, agricultural, and living wastewater have posed a serious danger to water security in recent years. The production of colours, medications, pigments, insecticides, wood preservatives, and rubber compounds frequently uses 4-nitrophenol (4-NP), a common water pollutant [1-5]. Even in tiny amounts, 4-NP can cause serious harm to aquatic life and

green plants in surface waters. A fundamental chemical process called hydrogenation of nitroarenes, such as 4-nitrophenol, to produce the equivalent aromatic amines is used to both synthesize anilines and remove hazardous nitro aromatics from aqueous solutions [6-10]. Moreover, aromatic amines such as aniline are essential components in the synthesis of methylene diphenyl diisocyanate. Methylene

^a Department of Chemistry, Faculty of Science and Technology, University of Kinshasa, Kinshasa, Democratic Republic of Congo.

^b Department of Chemistry, Pandit Deendayal Upadhyaya Adarsha Mahavidyalaya, Eraligool-788723, Karimganj, Assam, India.

^c Department of Chemistry, Shillong College, Boyce Road, Laitumkrah, Shillong-793003, Meghalaya, India. *Corresponding author. E-mail: sunshinekurbah@yahoo.com

diphenyl diisocyanate is an essential component in the synthesis of polyurethanes, a class of speciality polymers used in many industries, such as the building and furniture sectors, where it is used to make foams and insulations, respectively [11-13]. The scientific community attempted to create alternative protocols for the reduction of aromatic nitro compounds in an effort to address the previously mentioned shortcomings. These protocols included the use of various reducing agents, such as hydrazine, silane, and sodium borohydride, in conjunction with catalysts for Cu, Pd, Au, Ru, Ag, and, more recently, Co and Ni [14-20]. Noble metal systems do, however, have certain inherent issues, such as high cost, metal nanoparticle interparticle aggregation, lack of reuse, and other flaws that prevent their widespread commercialization [21-23].

Thus, the development of more affordable, stable, reusable, and noble metal-free catalysts is still required. Replacing precious metals with widely available transition metals is a promising approach for reducing manufacturing expenses and promoting the conservation of precious metals on Earth. In this regard, lately, because of their affordability, nickel catalysts have been used in various organic processes, especially hydrogenations. Nickel-based catalysts offer a substitute for the hydrogenation of nitrobenzene because of its plentiful on Earth, with a relatively low cost and toxicity [24-28]. Despite their superior catalytic performance, the development of such nanostructured materials catalysts involves the use of costly organic functional ligands and metal supports. Among various kinds of supported Ni catalysts, carbon material supported Ni catalysts generated from biomass have attracted a lot of attention and widely studied to address this problem [29-31]. Renewable sourced metal-supported carbon catalysts that hydrogenate nitroarenes to anilines have made some headway. Recently lignin residue derived carbon supported cobalt, ruthenium and nickel catalysts generated from biomass for selective hydrogenation processes has been reported. This information served as a stimulus to start looking for fresh, renewable, and sustainable sources of carbon [32-35]. Motivated by the above mentioned studies and our understanding of the significance of biomass utilization in catalyst manufacture, we opted for lignin residue as a substitute carbon source. Remarkably, there are only few studies discussing the use of catalysts produced from lignin for organic conversions. In this paper, we report the synthesis, and characterization of biomass derived carbon supported nickel nanoparticles and explore their catalytic activity for reduction of aromatic nitro groups.

2. Material and Methods

2.1. Chemicals and Instruments

Solvents were reagent grade purchased from HiMedia, Sigma Aldrich. Other chemicals such as nitrobenzene, nickel nitrate hexahydrate ($\text{Ni}(\text{NO}_3)_2 \cdot 6\text{H}_2\text{O}$, (Sigma, 99.99%), sodium borohydride (NaBH_4 , Sigma, 99%), all chemicals were reagents grade and were used without further processing or purification. Powder XRD was recorded in a Bruker D8 Discover X-ray diffractometer, equipped with a LynxEye detector, using an acrylic sample holder. The ^1H NMR and ^{13}C NMR spectra were recorded on AMX-400 MHz and 100 MHz in DMSO-d_6 solution using TMS as internal standard. The morphologies of the NiO@LBM were characterized using scanning electron microscope (JSM-6360, Joel, with oxford EDS detector) operating at 1-30 kV. For sample preparation, diluted sample was put into the thin aluminum sheet by using

capillary tube and then allowing it to dry in air. The sample was also coated with a thin layer of gold before the experiment to minimize sample charging.

2.2. Procedure for the preparation of lignin residue

Soda lignin underwent a hydrothermal treatment to yield lignin residue [34]. Typically, a 100 mL batch autoclave was filled with 60 mL of distilled water and 5 g of soda lignin. After that, the autoclave was heated in an oil bath and stirred constantly for four hours while the reaction temperature was raised to 200 °C. The reactor was allowed to cool to ambient temperature once the reaction was finished, and unconverted soda lignin was easily removed from the bio-oil using simple filtration method. The lignin residue was dried in the oven at 120 °C for 8 hr.

2.3. Synthesis of NiO@Lignocellulosic biomass (NiO@LBM)

In a typical synthesis of NiO@LBM, $\text{Ni}(\text{NO}_3)_2 \cdot 6\text{H}_2\text{O}$ (0.58 g, 2.0 mmol) was dispersed in 30 mL deionized water for 30 minutes. To this solution, lignocellulosic biomass (2 g) stirred in 10 mL deionized water was added, and stirred at room temperature. The reaction mixture was then heated at 150 °C to dryness for 4 hr. Finally, the prepared NiO@LBM nanoparticle was heated in a muffle furnace at the rate of 5 °C min^{-1} under air conditions until reaching 700 °C and held at this temperature for 6 hr. The resulting black grey powder obtained was kept for further use.

2.4. General procedure for the catalytic hydrogenation of nitroarene

In a typical reaction, nitroarene (2.0 mmol) and NiO@LBM (2.0 mg) were mixed in water (10 ml) and the reaction mixture was stirred at room temperature for 3 minutes. Subsequently, NaBH_4 (3.0 mol) was added to the reaction vessel and the reaction mixture was stirred at 23 °C for the required time. The completion of reactions was monitored by thin layer chromatography (TLC) and gas chromatography (GC). The catalyst was separated from the reaction mixture by simple filtration, after the completion of each and every reaction. The crude products obtained were extracted with ethyl acetate/hexane mixtures (5:1) and dried over anhydrous sodium sulfate (Na_2SO_4). The products were purified with column chromatography using 20% ethyl acetate/hexane as eluent. The products were confirmed by ^1H and ^{13}C NMR spectroscopy. The yields of products were calculated using gas chromatography (GC) and column chromatography.

3. Results and Discussion

3.2. Characterization of NiO@LBM

Lignocellulosic materials, also known as lignocellulosic biomass, are among the most abundant and readily available renewable resources. The constituent material of the plant that forms the cell wall is called lignocellulosic biomass, and it is composed of several kinds of macromolecules with a variable chemical composition. Lignin is the primary source of aromatic polymers in the environment and containing phenolic groups which serves as an excellent absorber of nickel nitrate. The method for the preparation of the NiO@LBM catalyst is highlighted in **Scheme 1**. The preparative procedure involves two steps, in the first step it involved reaction of $\text{Ni}(\text{NO}_3)_2 \cdot 6\text{H}_2\text{O}$ with lignocellulosic biomass at room temperature and then heated at 150 °C to

dryness for 4 hr to generate NiO@LBM. In the next step, the prepared NiO@LBM was heated in a muffle furnace at the rate of 5 °C min⁻¹ under air conditions until reaching 700 °C for 6 hr. The protocol adopted in the preparation of NiO@LBM is a low-cost strategy, simple and environmental friendly. To understand the performance of newly synthesized NiO@LBM

nanoparticle for catalytic hydrogenation of nitroarenes, we characterized the catalyst by transmission electron microscopy (TEM), EDX, and X-ray diffraction (XRD). The structures and morphology of the synthesized materials was determined by TEM studies.



Scheme 1. Schematic illustration of the synthesis of NiO@LBM nickel nanoparticles.

The powder XRD pattern of NiO@LBM nanoparticles is shown in Figure 1. Three peaks at 43.21°, 51.69° and 62.47.5° were clearly seen in the XRD patterns of the NiO@LBM nanoparticles, these peaks corresponded to crystalline facets of Ni (111), Ni (200), and Ni (220), respectively [34, 35]. By examining the full width at half maximum (FWHM) value of the XRD spectra, one might study the crystal quality and the distribution of compositional phases of the formed structure. Therefore, the Debye-Scherrer equation is used to determine the average crystallite size from the XRD measurement.

$$D = \frac{0.95\lambda}{\beta \cos\theta}$$

where λ is wave length of the incident X-ray (0.154 nm), θ is the Bragg's angle and β is full width at half maximum (FWHM), and D is the average crystallite size (diameter). Additionally, the above equation yielded an average crystallite diameter of about 10.64 nm.

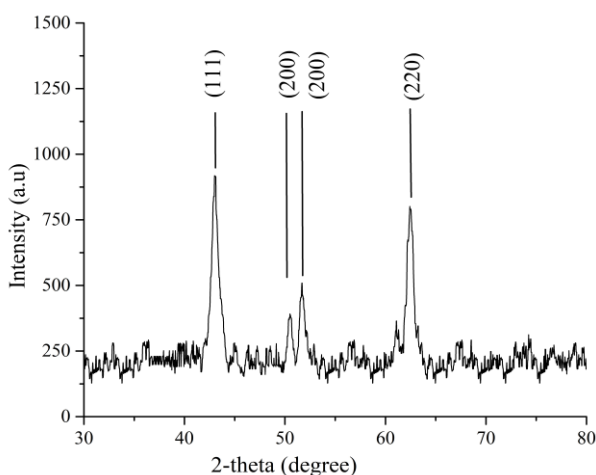


Fig. 1. XRD pattern of the newly synthesized NiO@LBM.

The energy dispersive X-ray (EDX) analysis of NiO@LBM nanocrystallites showed an optical absorption peak at 0.8 keV

and 7.6 keV approximately, which is the characteristics absorption peak of nickel nanoparticles (Figure S1). Similarly, the EDX spectrum of NiO@LBM shows maximum percentage of nickel with 47%, oxygen 30% and carbon with 21%. The overall characterization provides information about the crystallinity, uniform morphology and remarkable phase purity of NiO@LBM. The Transmission Electron Microscope (TEM) of NiO@LBM and SEAD pattern is shown in Figure 2. The TEM image shows that the particles are irregular in shape, in which the particles aggregate together. The particle size distribution of NiO@LBM nanoparticles is shown in Figure. 2 (d) and the average size of nickel nanoparticles was calculated and found to be 7.5 nm.

The catalytic reduction of nitrobenzene was chosen as the model substrate to study the catalytic activity of the newly synthesized NiO@LBM. In our initial investigations we carried out the catalytic reaction by observing the effect of the catalyst concentration. We discovered that increasing the amount of catalyst from 0.5 mg to 1.0 mg resulted in the greatest yield (Table 1, entry 12). The yield generated fell when the amount of NiO@LBM was reduced, and contrary to expectations (Table 1, entry 11), the yield declined as the amount of NiO@LBM increased from 2.5-3.0 mg (Table 1, entries 13–16). Hence, the optimal catalyst concentration for the present catalytic system was 1.0 mg and increasing the concentration beyond this limit may have negative impact such as catalyst aggregation or inhibition. The catalytic reduction of nitrobenzene was examined using different types of organic solvents, and the findings were presented in Table 1. It is clear that using water as a medium facilitates a smooth response (Table 1, Entry 12). Table 1 shows the findings of our study on the effects of temperature and reducing agents. With NaBH₄ as a reducing agent at room temperature, which produced the equivalent aniline with 85% conversion, the most favorable findings were achieved (Table 1, Entry 12). Changing the reaction parameters has significant influence on the process of conversion of the intended products. The outcomes of our investigation confirmed that the current method increased activity.

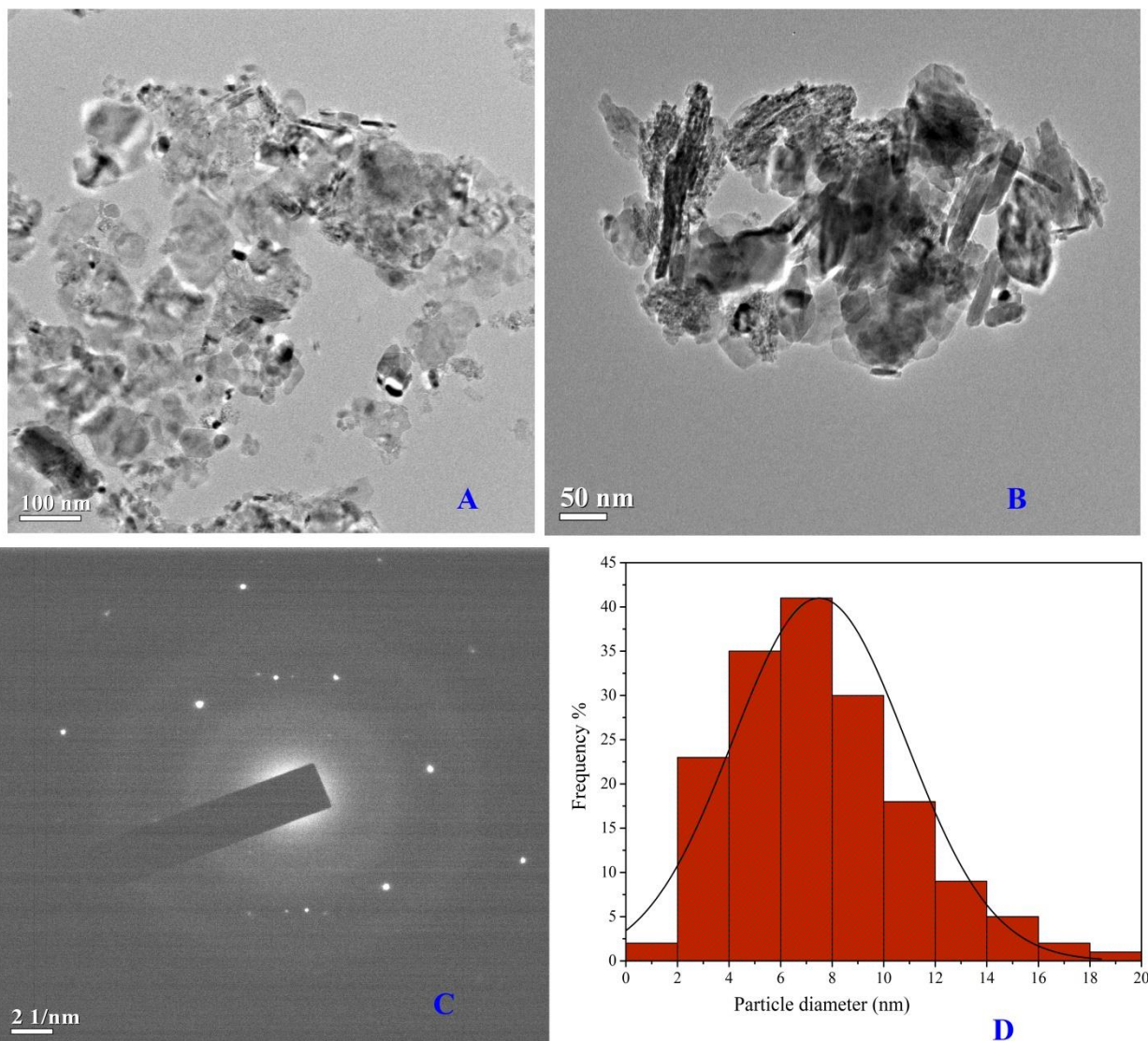
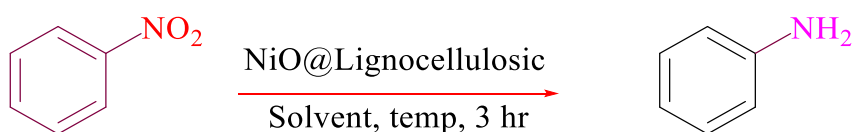


Fig. 2. (a-b) TEM image of NiO@LBM nanoparticle, (c) SAED pattern of NiO@LBM and (d) Particles size distribution.

Table 1. Optimization of reaction conditions for the catalytic reduction of nitrobenzene to aniline using NiO@Lignocellulosic.^a



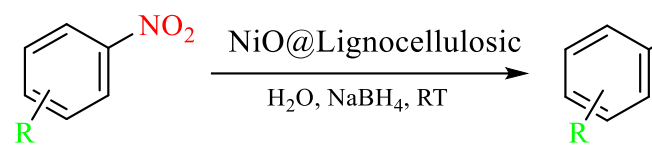
| Entry | Catalyst | Reducing agents | Solvents | Temp (°C) | Yield (%) ^b |
|-------|----------|-------------------|----------------------------------|-----------|------------------------|
| 1 | 1 mg | NaBH ₄ | CH ₃ OH | RT | 63 |
| 2 | 1 mg | NaBH ₄ | C ₂ H ₅ OH | RT | 68 |
| 3 | 1 mg | NaBH ₄ | CH ₃ CN | RT | 31 |
| 4 | 1 mg | NaBH ₄ | Toluene | RT | 17 |
| 5 | 1 mg | NaBH ₄ | DMF | RT | 48 |
| 6 | 1 mg | NaBH ₄ | DMSO | RT | 57 |
| 7 | 1 mg | NaBH ₄ | H ₂ O | 50 | 80 |
| 8 | 1 mg | NaBH ₄ | H ₂ O | 75 | 78 |
| 9 | 1 mg | NaBH ₄ | H ₂ O | 100 | 74 |
| 10 | 0.0 mg | NaBH ₄ | H ₂ O | RT | 11 |
| 11 | 0.5 mg | NaBH ₄ | H ₂ O | RT | 76 |
| 12 | 1 mg | NaBH ₄ | H ₂ O | RT | 85 |
| 13 | 1.5 mg | NaBH ₄ | H ₂ O | RT | 78 |
| 14 | 2.0 mg | NaBH ₄ | H ₂ O | RT | 71 |
| 15 | 2.5 mg | NaBH ₄ | H ₂ O | RT | 65 |
| 16 | 3.0 mg | NaBH ₄ | H ₂ O | RT | 57 |

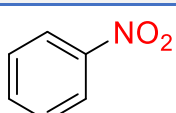
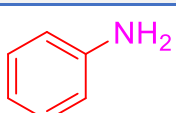
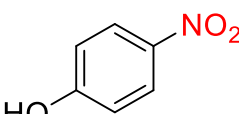
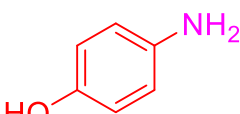
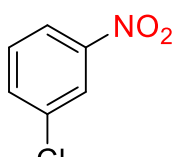
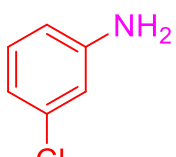
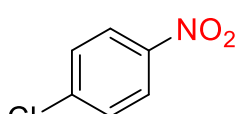
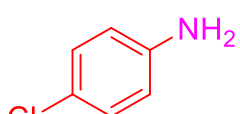
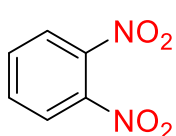
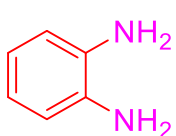
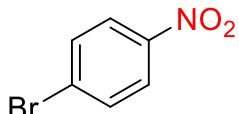
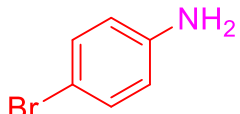
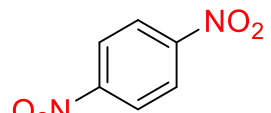
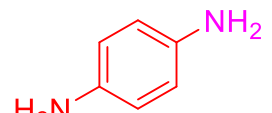
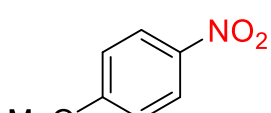
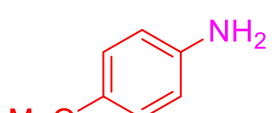
^aReaction conditions: Substrate (2.0 mmol), catalyst (1.0 mg), Reducing agents (3.0 mmol), solvent (10 mL), temperature (RT). ^bIsolated yield after chromatography.

We investigate the catalyst-induced reduction various aromatic nitro compounds in order to examine the broadness of substrates and the viability of the current catalytic system. The reduction reaction was performed out using the standardized procedure, NiO@LBM (as a catalyst), NaBH₄ and water as a solvent at room temperature for 4 hr (Table 2). It is essential to hydrogenate halonitroarenes to produce corresponding haloanilines because haloanilines are extensively utilised in dyes, agrochemicals, pharmaceuticals, and polymers. Catalytic hydrogenation of 4-nitrophenol give 4-aminophenol with 96% yield, similarly hydrogenation of 1-chloro-3-nitrobenzene and 1-chloro-4-nitrobenzene to corresponding, 3-chloroaniline (95%) and 4-chloroaniline with 96% was successfully achieved (Table 2, entries 2-4). Benzene bearing two nitro groups such as 1,2-dinitrobenzene and 1,4-

dinitrobenzene undergo hydrogenation smoothly giving benzene-1,2-diamine benzene-1 with 90% yield and 1,4-diamine with 93% yield, respectively (Table 2, entries 5, 7). Similarly, hydrogenation of 1-bromo-4-nitrobenzene giving 4-bromoaniline with 94%, 1-fluoro-4-nitrobenzene giving 4-fluoroaniline with 93% and 1-iodo-4-nitrobenzene giving 4-iodoaniline with 90%, respectively (Table 2, entries 6, 9 and 10). Also, nitroarene containing functional groups like methoxy group and nitrile was successfully reduced to corresponding 4-methoxyaniline (90%) and 4-aminobenzonitrile with 92%, respectively (Table 2, entries 8, 11). The excellent compatibility of this nickel-catalyzed selective hydrogenation of the nitro group motivated us to investigate its effectiveness for reducing pharmaceuticals, dyes, agrochemicals, and polymers in the later stages.

Table 2. Reduction of aromatic nitroarenes to aniline using NiO@Lignocellulosic.^a



| Entry | Reactant | Product | Yield ^b /% |
|-------|---|--|-----------------------|
| 1 |  |  | 98 |
| 2 |  |  | 96 |
| 3 |  |  | 95 |
| 4 |  |  | 96 |
| 5 |  |  | 90 |
| 6 |  |  | 94 |
| 7 |  |  | 93 |
| 8 |  |  | 90 |

| | | |
|----|--|----|
| 9 | | 93 |
| 10 | | 90 |
| 11 | | 92 |

^aStandard reaction conditions: Substrate (2.0 mmol), catalyst (1.0 mg), NaBH₄ (3.0 mmol), solvent (10 mL), temperature (RT). ^bIsolated yield after chromatography.

4. Conclusions

In conclusion, we have synthesized a lignocellulosic biomass derived carbon supported nickel nanoparticles. The catalytic hydrogenation of nitroarenes has been studied using the NiO@LBM nanocatalyst. This study may offer a new strategy for the rational design and application of NiO@LBM nanomaterial for catalytic hydrogenation of nitroarenes. Moreover, the entire process is straightforward and operates in an eco-friendly manner, making the current approach highly desirable as it provides intriguing possibilities for the catalytic reduction of aromatic nitro compounds to aromatic amines.

Supporting Information

EDS spectrum of NiO@LBM and NMR spectra (¹H and ¹³C) of the anilines.

Acknowledgments

Authors would like to thank Head SAIF, North-Eastern Hill University, Shillong-793022, India, for providing TEM, EDX, ¹H and ¹³C NMR spectra.

Author Contributions

Conceptualization, S.D.K., K.U., N.S.C.; Methodology, S.D.K., K.U., N.S.C.; Investigation and Formal Analysis, S.D.K., K.U., N.S.C.; Software, S.D.K., N.S.C.; Resources, S.D.K., K.U., N.S.C.; Supervision, S.D.K.; Validation, S.D.K., K.U., N.S.C.; Visualization, S.D.K., K.U.; Writing Original Draft, S.D.K., K.U.; Writing – Review and Editing, S.D.K., K.U., N.S.C. All authors have read and agreed to the published version of the manuscript.

References and Notes

- [1] Smith, A. M.; Whyman, R. *Chem. Rev.* **2014**, *114*, 5477. [\[Crossref\]](#)
- [2] Bullock, R. M. *Science*, **2013**, *342*, 1054. [\[Crossref\]](#)
- [3] Li, H.; Gan, S.; Han, D.; Ma, W.; Cai, B.; Zhang, W.; Zhang, Q.; Niu, L. *J. Mater. Chem. A*. **2014**, *2*, 3461. [\[Crossref\]](#)
- [4] Liew, K. H.; Rocha, M.; Pereira, C.; Pires, A. L.; Pereira, A. M. *ChemCatChem*. **2017**, *9*, 3930. [\[Crossref\]](#)
- [5] Baranwal, K.; Dwivedi, L. M.; Singh, V. *Int. J. Biol. Macromol.* **2018**, *120*, 2431. [\[Crossref\]](#)
- [6] Bhatti, Z. I.; Toda, H.; Furukawa, K. *Water. Res.* **2002**, *36*, 1135. [\[Crossref\]](#)
- [7] Duan, Y.; Song, T.; Dong, X.; Yang, Y. *Green Chem.* **2018**, *20*, 2821. [\[Crossref\]](#)
- [8] Murugesan, K.; Senthamarai, T.; Chandrashekhar, V. G.; Natte, K.; Kamer, P. C. J.; Beller, M. R. V. *Chem. Soc. Rev.* **2020**, *49*, 6273. [\[Crossref\]](#)
- [9] Li, X.; Gao, W.; Li, L.; Li, B.; Chen, M.; Ge, Y.; Liu, S.; Wang, L.; Ma, L.; Niu, L.; Li, Y.; Liu, Z.; Chen, J. *ACS Appl. Nano Mater.* **2024**, *7*, 14540. [\[Crossref\]](#)
- [10] Jagadeesh, R. V.; Surkus, A. E.; Junge, H.; Pohl, M. M.; Radnik, J.; Rabeah, J.; Huan, H.; Schunemann, V.; Bruuckner, A.; Beller, M. *Science*, **2013**, *342*, 1073. [\[Crossref\]](#)
- [11] Orlandi, M.; Brenna, D.; Harms, R.; Jost, S.; Benaglia, M. *Org. Proc. Res. Dev.* **2018**, *22*, 430. [\[Crossref\]](#)
- [12] Pocock, E.; Diefenbach, M.; Hood, T. M.; Nunn, M.; Richards, E.; Krewald, V.; Webster, R. L. *J. Am. Chem. Soc.* **2024**, *146*, 19839. [\[Crossref\]](#)
- [13] Martina, K.; Moran, M. J.; Manzoli, M.; Trukhan, M. V.; Kuhn, S.; Gerven, T. V.; Cravotto, G. *Org. Proc. Res. Dev.* **2024**, *28*, 1515. [\[Crossref\]](#)
- [14] Duan, Z.; Ma, G.; Zhang, W. *Bull. Korean Chem. Soc.* **2012**, *33*, 4003. [\[Crossref\]](#)
- [15] Kyungsoon, K.; Woonphil, B.; Sunghwan, O. *J. Korean Chem. Soc.* **1995**, *39*, 812.
- [16] Formenti, D.; Ferretti, F.; Scharnagl, F. K.; Beller, M. *Chem. Rev.* **2019**, *119*, 2611. [\[Crossref\]](#)
- [17] Han, B. H.; Shin, D. H.; Lee, H. R. *J. Korean Chem. Soc.* **1989**, *33*, 577.
- [18] Yin, Z.; Xiao, Y.; Wan, X.; Jiang, Y.; Chen, G.; Shi, Q.; Cao, S. *J. Mater. Sci.* **2021**, *56*, 3874. [\[Crossref\]](#)
- [19] Zhang, F.; Zhao, C.; Chen, S.; Li, H.; Yang, H.; Zhang, X. M. *J. Catal.* **2017**, *348*, 212. [\[Crossref\]](#)
- [20] Bai, X.; Gao, Y.; Liu, H.; Zheng, L. *Phys. Chem. C*. **2009**, *113*, 17730. [\[Crossref\]](#)
- [21] Wu, H.; Huang, X.; Gao, M.; Liao, X.; Shi, B. *Green Chem.* **2011**, *13*, 651. [\[Crossref\]](#)
- [22] Layek, K.; LakshmiKantam, M.; Shirai, M.; Hamane, D. N.; Sasaki, T.; Maheswaran, H. *Green Chem.* **2012**, *14*, 3164. [\[Crossref\]](#)
- [23] Sarki, N.; Kumar, R.; Singh, B.; Ray, A.; Naik, G.; Natte, K.; Narani, A. *ACS Omega* **2022**, *7*, 19804. [\[Crossref\]](#)

- [24] Kondeboina, M.; Enumula, S. S.; Gurram, V. R. B.; Yadagiri, J.; Burri, D. R.; Kamaraju, S. R. R. *New. J. Chem.* **2018**, 42, 15714. [\[Crossref\]](#)
- [25] Lu, X.; He, J.; Jing, R.; Tao, P.; Nie, R.; Zhou, D.; Xia, Q. *Sci. Rep.* **2017**, 7, 2676. [\[Crossref\]](#)
- [26] Nakatsuka, K.; Yoshii, T.; Kuwahara, Y.; Mori, K.; Yamashita, H. *Chem. Eur. J.* **2018**, 24, 898. [\[Crossref\]](#)
- [27] Romanazzi, G.; Fiore, A. M.; Mali, M.; Rizzuti, A.; Leonelli, C.; Nacci, A.; Mastroilli, P.; Dell'Anna, M. M. *Mol. Catal.* **2018**, 446, 31. [\[Crossref\]](#)
- [28] Budi, C. S.; Saikia, D.; Chen, C. S.; Kao, H. M. *J. Catal.* **2019**, 370, 274. [\[Crossref\]](#)
- [29] Lam, E.; Luong, J. H. T. *ACS Catal.* **2014**, 4, 3393. [\[Crossref\]](#)
- [30] Varma, R. S. *ACS Sustainable Chem. Eng.* **2019**, 7, 6458. [\[Crossref\]](#)
- [31] Abdullah, S. H. Y. S.; Hanapi, N. H. M.; Azid, A.; Umar, R.; Juahir, H.; Khatoun, H.; Endut, A. *Renew. Sustain. Energy. Rev.* **2017**, 70, 1040. [\[Crossref\]](#)
- [32] Veerakumar, P.; Muthuselvam, I. P.; Hung, C. T.; Lin, K. C.; Chou, F. C.; Liu, S. B. *ACS Sustainable Chem. Eng.* **2016**, 4, 6772. [\[Crossref\]](#)
- [33] Song, T.; Ren, P.; Duan, Y.; Wang, Z.; Chen, X.; Yang, Y. *Green Chem.* **2018**, 20, 4629. [\[Crossref\]](#)
- [34] Kumar, A.; Goyal, V.; Sarki, N.; Singh, B.; Ray, A.; Bhaskar, T.; Bordoloi, A.; Narani, A.; Natte, K. *ACS Sustainable Chem. Eng.* **2020**, 8, 15740. [\[Crossref\]](#)
- [35] Schreifels, J. A.; Maybury, P. C.; Swartz, W. E. *Org. Chem.* **1981**, 46, 1263. [\[Crossref\]](#)

How to cite this article

Kurbah, S. D.; Umdor, K.; Clovis, N. S. *Orbital: Electronic J. Chem.* **2024**, 16, 286. DOI: <http://dx.doi.org/10.17807/orbital.v16i4.21957>